J. Plasma Phys. (2021), *vol*. 87, 885870301
Published by Cambridge University Press
doi:10.1017/S0022377821000490

Bispectral analysis of broadband turbulence and geodesic acoustic modes in the T-10 tokamak

Greg A. Riggs [1], S.H. Nogami [1], M.E. Koepke [1,†], A.V. Melnikov [2,3,4], L.G. Eliseev [2], S.E. Lysenko [2], P.O. Khabanov [2,4], M.A. Drabinskij [2,4], N.K. Kharchev [2,5], A.S. Kozachek [6], M.V. Ufimtsev [7] and HIBP Team [6]

[1]Department of Physics and Astronomy, West Virginia University, Morgantown, WV 26505, USA

[2]National Research Centre 'Kurchatov Institute', Moscow 123182, Russian Federation

[3]National Research Nuclear University MEPhI, Moscow 115409, Russian Federation

[4]Moscow Institute of Physics and Technology, Dolgoprudny 141700, Russian Federation

[5]Prokhorov General Physics Institute, RAS, Moscow 117942, Russian Federation

[6]Institute of Plasma Physics, NSC KIPT, Kharkov 310108, Ukraine

[7]Department of Computational Mathematics and Cybernetics, Moscow State University, Moscow 119991, Russian Federation

(Received 14 July 2020; revised 26 April 2021; accepted 28 April 2021)

Local fluctuations of electrostatic potential, poloidal electric field, magnetic potential and electron density are simultaneously measured in the T-10 tokamak by a heavy ion beam probe (HIBP) having a five-slit energy analyser, which allows an estimate of the turbulent particle flux and $\boldsymbol{E} \times \boldsymbol{B}$ rotation velocity in the off-minor-axis gradient zone of the toroidal plasma column. The high spatial and temporal resolution of the modern multichannel HIBP makes it an effective tool to study plasma oscillations. Motivated by previous work that has documented time-resolved interactions between measured plasma parameters using correlation analysis (coherence of $E_{\rm pol}$ and density n_e, and cross-phase), a new result from bicorrelation analysis (bicoherence of magnetic potential A_ζ and density n_e, and biphase) is reported for documenting the evidence of wave–wave coupling and energy transfer associated with the interaction between geodesic acoustic modes (GAM) and broadband, quasi-coherent modes.

Key words: plasma nonlinear phenomena

1. Motivation for 'frontiers' and 'fusion' scientific collaboration

Fusion research is driven by the applied goal of energy production from fusion reactions. There is, however, a wealth of 'frontier' physics to be discovered and studied along the way. This paper discusses the topic of zonal flow, a phenomenon originally identified in the formation of the solar tachocline and stellar differential rotation, which is now considered a mechanism for the flow-shear-induced formation of transport barriers and associated transition of magnetic-confinement regimes in fusion (Melnikov 2016). Promoting scientific collaboration with fusion science can advance plasma physics

† Email address for correspondence: Mark.Koepke@mail.wvu.edu

frontiers and vice versa. Research by 'frontiers' professors using fusion-oriented facilities has led to valuable insights and shared tools, has advanced the pursuit and understanding of fundamental plasma physics, has widened the scope of the plasma science and fusion research fields, and has generated ideas from cross-fertilizing between 'frontiers' and 'fusion'. Here, the geodesic acoustic mode (GAM), a high-frequency branch of zonal flow, is intensively studied in T-10 tokamak (Melnikov *et al.* 2006, 2015*a*,*b*) because it is potentially important as a turbulence self-regulating mechanism (Diamond *et al.* 2005). Researchers using the T-10 tokamak, TJ-II stellarator, DIII-D tokamak, Texas Helimak and West Virginia University (WVU) Q Machine collaborated in this study.

Using bispectral analysis of HIBP data in the core plasmas, Melnikov *et al.* (2017*b*) investigated the interaction between GAM and quasi-coherent turbulence, which demonstrated the existence of statistically significant auto- and cross-bicoherence at the GAM frequency that suggests wave–wave coupling. The results revealed details of the three-wave interaction between GAM and broadband electrostatic turbulence. Experiments were performed at the T-10 circular tokamak, located in the National Research Centre of Kurchatov Institute, Moscow, Russia. WVU was invited to collaborate to independently assess and confirm the correlation analysis and the bispectral analysis. Here, the interaction of GAM with ambient turbulence in T-10 (Eliseev *et al.* 2018) is re-investigated using a functionally similar bicoherence analysis to quantify not only the coupling, but also the energy transfer, between local fluctuations in the magnetic potential A_ζ, electron density n_e and electrostatic potential ϕ. The intention is to confirm or refine previous bicoherence interpretations (Melnikov *et al.* 2017*a*) and determine the wave–wave energy transfer direction. Findings confirm that the GAM frequency is significantly involved in three-wave interactions between the narrowband GAM at 17 kHz and the broadband turbulence at higher frequency. Findings also confirm that the degree of coupling between ϕ and either n_e or A_ζ fluctuations is weaker than that between n_e and A_ζ. Findings refine the picture of energy transfer by establishing the transfer direction between the local fluctuations and identifying multi-signature consistency within subsets of biphase.

2. Broadband turbulence and GAM in the T-10 Tokamak

Gradients in density, temperature and pressure provide the main source of free energy for various linear instabilities. Broadband turbulence arises through nonlinear coupling between nonlinearly saturated instabilities. Increasing-frequency cascades and decreasing-frequency cascades can result in the viscous dissipation of energy at small scales and in the transfer of energy into larger scales, such as zonal flow and GAM. Energy can be removed from the broadband turbulence by dissipation through collisional and Landau damping.

Zonal flow is a flow-shear region structured into azimuthally symmetric bands having finite k_r, and having $n = m = 0$ electric field fluctuations. Zonal flow co-exists with microinstabilities. Zonal flow regulates turbulence-induced transport by shearing, and thus quenching, the underlying microinstability.

The GAM is an oscillating zonal flow observed mainly in the edge region of a tokamak plasma. It oscillates in the range 10–20 kHz with a frequency that is proportional to the sound velocity c_s divided by the tokamak major radius R (Fujisawa *et al.* 2007). By shearing the velocity profile, GAM can effect a reduction of turbulent transport and, thereby, become an important element of the turbulent system. The GAM is important to 'fusion' science because it factors into complex flow-shear regulation of interactions between plasma gradients, turbulence and flows, and the triggering of high-confinement equilibrium 'H-mode' (Conway *et al.* 2011; Cziegler *et al.* 2015; Melnikov 2019).

https://doi.org/10.1017/S0022377821000490 Published online by Cambridge University Press

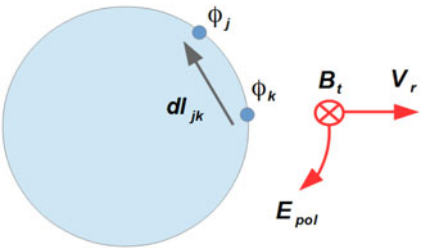

FIGURE 1. Outline of the electric field $E_{\rm pol}$ and radial velocity V_r measurement; ϕ_j and ϕ_k are potentials in sample volumes on the same flux surface, measured by slits #j and #k, respectively, at a distance dl_{jk}.

Broadband turbulence and GAM coexist in the T-10 tokamak. Figure 1 (consistent with figure 1 of Eliseev *et al.* 2018) diagrams the geometry of the poloidal electric field $E_{\rm pol}$ and velocity V_r measurements. Same-flux-surface potentials ϕ_j, ϕ_k are locally measured by slits j and k of the five-slit energy analyser, where $(j, k) = (1, 2), (2, 3), (3, 4)$, and $(4, 5)$ are commonly used. The inferred $E_{\rm pol} = (\phi_j - \phi_k)/dl_{jk}$, where dl_{jk} is the neighbour-slit separation.

Figure 6 of Eliseev *et al.* (2018), not shown here, graphs the 50–200 kHz frequency-integrated flux Γ through the various pairs of HIBP slits. The mean flux suddenly increases upon the transition of the discharge from the ohmic (OH) stage (2×10^{19} m^{-2} s^{-1}) to the electron cyclotron resonant heating (ECRH) stage (3×10^{19} m^{-2} s^{-1}) as a result of a significant increase in amplitude of fluctuations of both $E_{\rm pol}$ and density despite the decrease of coherence between those two quantities. In this report, as in Melnikov *et al.* (2017*a*) and Gryaznevich *et al.* (2020), bicoherence of the OH-stage fluctuations is presented. Specifically, we consider data collected from T-10 shot #62753, with relevant plasma parameters $I_p = 180$–250 kA and $\bar{n}_e = (1.2$–$1.4) \times 10^{19}$ m^{-3}.

3. Background

Local fluctuations of electrostatic potential, poloidal electric field, magnetic potential and electron density were simultaneously measured in the T-10 tokamak. The turbulent particle flux was measured in the plasma edge layer by multipin Langmuir probes, while inside the core plasmas, the flux was measured by multichannel HIBP (Dnestrovskij *et al.* 1994; Demers *et al.* 2001; Melnikov *et al.* 2017*b*).

The HIBP is a unique diagnostic tool that can acquire simultaneous information about the local plasma potential ϕ, plasma density n_e and toroidal magnetic potential A_ζ in the core area of toroidal plasmas (Dnestrovskij *et al.* 1994; Melnikov *et al.* 2017*b*). The diagnostic functions by passing a primary probing beam of ions through a hot plasma, which exposes the energetic (up to 300 keV) ions to a toroidal magnetic field (Melnikov *et al.* 2013); to ensure the resulting Larmor radius exceeds the plasma area, heavy ions (in this case, Tl^+) are used (Melnikov *et al.* 2017*b*). In transit, collisions with plasma particles lead to secondary ionization of a proportion of the beam ions. With knowledge of the initial kinetic energy $\mathcal{E}_b$ of the beam, measurement of the kinetic energy $\mathcal{E}_d$ of the secondary ions provides the local plasma potential as $\phi = (\mathcal{E}_d - \mathcal{E}_b)/e$ (Jobes & Hickock 1970). Additionally, the plasma density n_e may be inferred from the secondary beam current I_t (cf. (2)–(4) in Melnikov *et al.* 2010) and toroidal magnetic potential A_ζ is deduced from the toroidal beam shift ζ (cf. (7)–(10) in Melnikov *et al.* 2010).

We present analysis of the HIBP data to confirm the interpretations of Melnikov *et al.* (2017*a*). In particular, there was found to be statistically significant nonlinear coupling

https://doi.org/10.1017/S0022377821000490 Published online by Cambridge University Press

between fluctuations in density and fluctuations in magnetic potential (cf. figure 7*b* in Melnikov *et al.* 2017*a*), and to a lesser extent, evidence of nonlinear coupling between magnetic and electrostatic potential fluctuations (cf. figure 7*c* in Melnikov *et al.* 2017*a*). The detection of these nonlinear interactions, in conjunction with the associated energy transfer, is facilitated by cross-bicoherence analysis (Kim & Powers 1979; Kim, Beall & Powers 1980; Xu *et al.* 2009).

4. Analysis of wave–wave cross-bicoherence

The bispectrum is a two-dimensional (2-D) Fourier transform of the triple correlation function (Kim *et al.* 1980; Stauber 1995; Riggs 2020), which manifests as a triple product of Fourier components. Explicitly,

$$\mathcal{B}_{xyz}(f_1, f_2) = \left\langle \Phi_x(f_1)\Phi_y(f_2)\Phi_z^*(f_1+f_2) \right\rangle, \tag{4.1}$$

where angled brackets represent a time average over many realizations, and $\Phi_i(f)$ is a Fourier coefficient at frequency f, for time series i. For an individual peak in the bispectrum at (f_1, f_2), the sign of the real part $\mathrm{Re}(\mathcal{B}_{xyz})$ encodes information about the phase relationship between modes $\Phi_x(f_1)$, $\Phi_y(f_2)$ and $\Phi_z(f_1+f_2)$ (Stauber 1995, p. 11; Xu *et al.* 2009). This may be understood by considering the biphase θ or associated phase angle. For a single realization,

$$\theta_{xyz}(f_1, f_2) = \varphi_x(f_1) + \varphi_y(f_2) - \varphi_z(f_1+f_2), \quad -\pi < \theta < \pi, \tag{4.2}$$

where $\varphi_i(f)$ is the phase angle of $\Phi_i(f)$. If we consider quadratic coupling terms, parent modes and daughter modes have a triplet relationship recognized by parents at frequencies f_a and f_b, with daughters at the sum and difference frequencies $f_a \pm f_b$ (Stauber 1995, p. 8; Riggs 2020, p. 27; Stauber & Koepke 2021). In the special case $x = y = z$ (known as *auto*-bispectrum), parent–daughter interactions would produce bispectral peaks at (f_a, f_b), (f_b, f_a), $(f_a, f_b - f_a)$, $(f_b - f_a, f_a)$, $(-f_a, f_b)$, $(-f_b, f_a + f_b)$, $(f_a - f_b, f_b)$ and $(-f_a, f_a + f_b)$, where $f_b > f_a$. When associated with these peaks, $|\theta_{xxx}| < \pi/2$ or $\mathrm{Re}(\mathcal{B}_{xxx}) > 0$ corresponds to an in-phase daughter mode (with respect to the parents), while $|\theta_{xxx}| > \pi/2$ or $\mathrm{Re}(\mathcal{B}_{xxx}) < 0$ represents an out-of-phase daughter (Stauber 1995, p. 11; Stauber & Koepke 2021). This information can implicate the direction of energy transfer even in the more general case ($x \neq y \neq z$), as the rate of change of power in the mode $\Phi_z(f_1+f_2)$ owing to the nonlinear interaction among $\Phi_x(f_1)$, $\Phi_y(f_2)$ and $\Phi_z(f_1+f_2)$ is proportional to $\mathrm{Re}(\mathcal{B}_{xyz}(f_1, f_2))$ (Kim & Powers 1979; Stauber 1995, p. 10). Figure 2 illustrates how a triangular region in a map of $\mathrm{Re}(\mathcal{B}_{xxx})$ spans the pertinent 2-D range of all possible interactions with one of the triplets (f_1, f_2, f_1+f_2). Note how the triangular-pattern angles and orientations transform from region to region, and that prominent spectral features are repeated throughout the range of plotted frequencies. For example, features in region 'B' are mirrored in region 'C', with the addition of a vertical shift equal to the displacement of the point from the y-axis. This reference illustration is helpful when comparing and contrasting with quadrant representations in the literature, as *cross*-bispectra will, in general, break these symmetries. With this in mind, it is convenient to define the squared bicoherence spectrum,

$$b^2_{xyz}(f_1, f_2) = \frac{\left|\left\langle \Phi_x(f_1)\Phi_y(f_2)\Phi_z^*(f_1+f_2) \right\rangle\right|^2}{\left\langle \left|\Phi_x(f_1)\Phi_y(f_2)\right|^2 \right\rangle \left\langle |\Phi_z(f_1+f_2)|^2 \right\rangle}, \tag{4.3}$$

which normalizes bispectral values to the range [0, 1], and indicates the proportion of energy change arising from nonlinear coupling (Stauber 1995, pp. 14).

https://doi.org/10.1017/S0022377821000490 Published online by Cambridge University Press

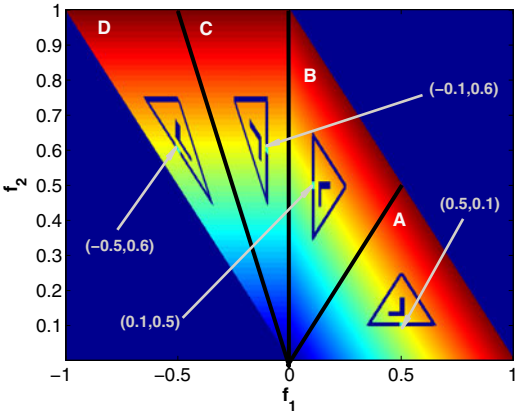

FIGURE 2. Visualization of symmetries implicit to the real part of the bispectrum (4.1) for real-valued time series, where $x = y = z$. Latin capitals and black lines are used to identify subregions of bi-frequency space, which will assist in assessment of upcoming figures. Axes have been normalized to Nyquist frequency; colour indicates how lines of constant sum frequency $f_3 = f_1 + f_2$ in quadrant I transform to lines of constant f_2 in quadrant II, through $f_2 = f_3 + (-f_1)$.

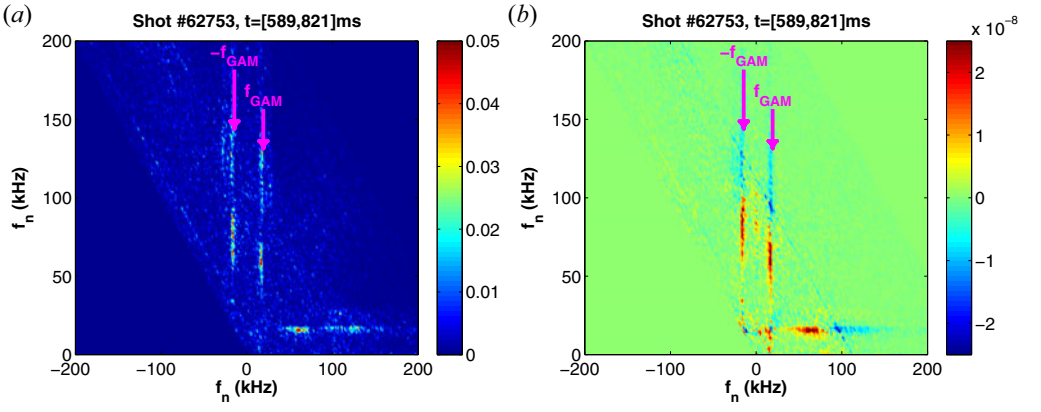

FIGURE 3. Bispectral analysis of OH plasma: (*a*) cross-bicoherence $b^2_{nn\zeta}$, (*b*) real part of bispectrum $\mathrm{Re}(\mathcal{B}_{nn\zeta})$. Notice lack of contribution from $f_\zeta = f_{\mathrm{GAM}}$ (subregion defined as 'D' in figure 2).

GAM, the only spectral feature at 17 kHz, plays a crucial role in the three-wave interaction that involves both upper- and lower-frequency halves of the higher-frequency broadband turbulence, as evidenced by the strong coupling apparent in multi-channel, HIBP measurements of turbulent particle flux and $\boldsymbol{E} \times \boldsymbol{B}$ rotation velocity in the gradient zone ($r/a = 0.8$) of the plasma column (Eliseev *et al.* 2018). Figure 3 shows cross-bicoherence $b^2_{nn\zeta}$ compared with the real part of the bispectrum $\mathrm{Re}(\mathcal{B}_{nn\zeta})$, which compactly illustrates both the extent and direction of energy transfer between plasma density fluctuations and magnetic potential fluctuations. In this case, wave energy is gained in the range 40–80 kHz, whereas wave energy is lost in the range 90–130 kHz. The frequency range of 40–150 kHz belongs to the quasicoherent (QC) modes in T-10, the specific type of oscillations under intensive study with various diagnostics (Vershkov *et al.* 2015, 2017). In figure 4, we compare line-outs of the cross-bicoherences $b^2_{nn\zeta}$

https://doi.org/10.1017/S0022377821000490 Published online by Cambridge University Press

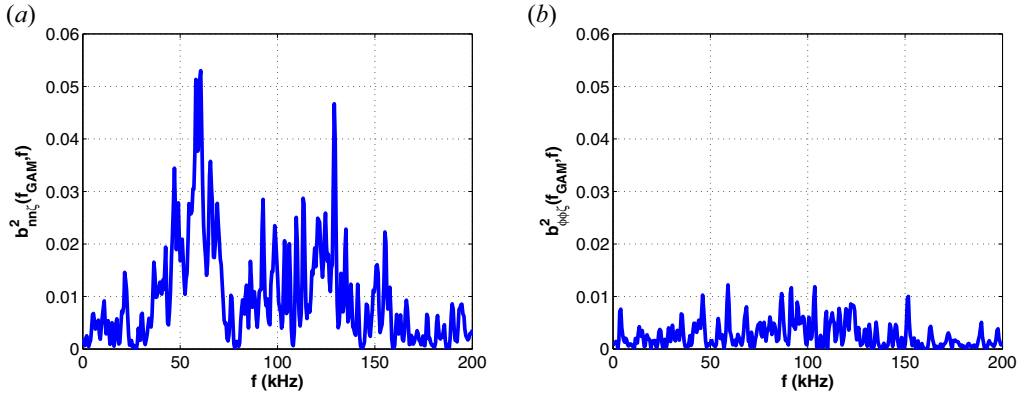

FIGURE 4. Comparing the nonlinear mode–mode coupling found in line-out of (*a*) $b^2_{nn\zeta}$ and (*b*) $b^2_{\phi\phi\zeta}$ at GAM frequency (as indicted in figure 3*a*), the latter is significantly weaker than the former. This implies the coupling between A_ζ and n_e is strongest and most informational (see figure 7).

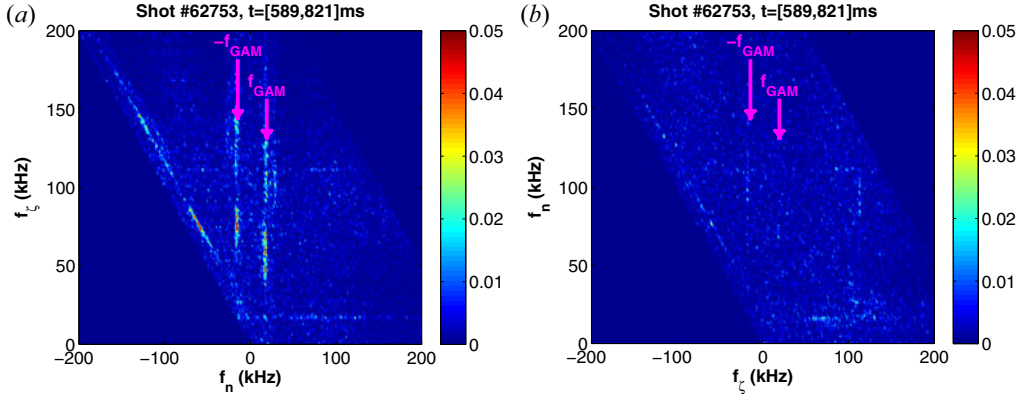

FIGURE 5. Bispectral analysis of OH plasma: (*a*) cross-bicoherence $b^2_{n\zeta n}$, (*b*) cross-bicoherence $b^2_{\zeta n\phi}$. Note lack of significant nonlinear coupling when electrostatic potential is included; additionally, compare regions 'A' and 'D' in figure 3(*a*) (as dictated by figure 2) with their respective counterparts in (*a*).

and $b^2_{\phi\phi\zeta}$ at $f_1 = f_{\mathrm{GAM}}$, where statistically significant values are observed in $b^2_{nn\zeta}$ (but not $b^2_{\phi\phi\zeta}$). This demonstrates the quantitative differences between electrostatic potential and density fluctuations, with regard to their coupling and energy exchange with the magnetic potential. Specifically, significant three-wave coupling is suggested in n, n, ζ bispectra, whereas it is weak in ϕ, ϕ, ζ bispectra. This independently reinforces the interpretation that density fluctuations, not potential fluctuations, exhibit more pronounced nonlinear wave–wave coupling (cf. figure 7*b*,*c* in Melnikov *et al.* 2017*a*). Additionally, the cross-bicoherence $b^2_{n\zeta n}$ (figure 5*a*) and its line-out at $f_1 = f_{\mathrm{GAM}}$ (figure 6*b*) affirm the importance of magnetic potential fluctuations in the context of this nonlinear coupling. Notably, the cross-bicoherence $b^2_{\zeta n\phi}$ displayed in figure 5(*b*) reiterates the diminished role of electrostatic potential fluctuations.

https://doi.org/10.1017/S0022377821000490 Published online by Cambridge University Press

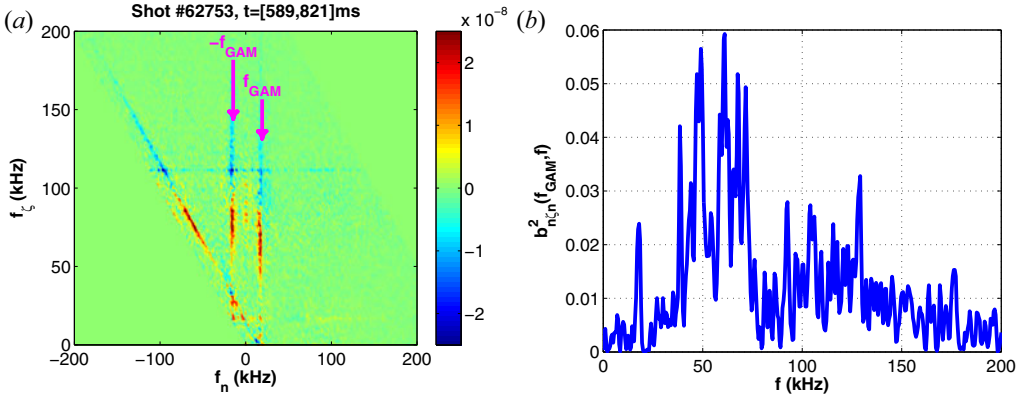

FIGURE 6. Further analysis: (*a*) real part of bispectrum $\mathrm{Re}(\mathcal{B}_{n\zeta n})$, (*b*) line-out of $b^2_{n\zeta n}$ at GAM frequency. These imply density and magnetic potential fluctuations are involved in complementary interactions with GAM.

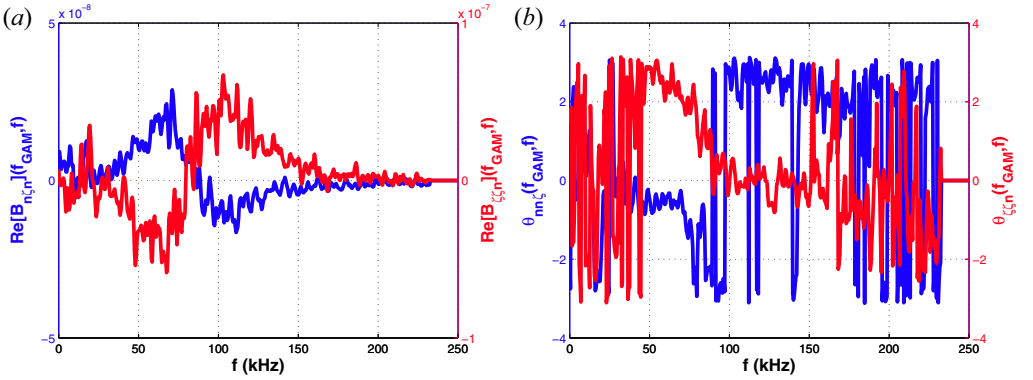

FIGURE 7. Analysis of energy transfer in OH plasma: (*a*) comparison of line-outs of $\mathrm{Re}(\mathcal{B}_{\zeta\zeta n})$ and $\mathrm{Re}(\mathcal{B}_{n\zeta n})$, (*b*) comparison of cross-biphases $\theta_{nn\zeta}$ and $\theta_{\zeta\zeta n}$ along GAM frequency. Remarkably, these quantities are approximately 180° out of phase across the entire frequency range of interest.

Naturally, we check the cross-bispectrum $\mathcal{B}_{\zeta\zeta n}$ to assure our assessment of energy transfer is valid. The distributions of $\mathrm{Re}(\mathcal{B}_{\zeta\zeta n})$ and $\mathrm{Re}(\mathcal{B}_{n\zeta n})$ along the GAM frequency ($f_1 \sim 17$ kHz) displayed in figure 7(*a*) are clearly complementary. In conjunction, figure 7(*b*) documents the approximately 180° phase difference between the cross-biphases $\theta_{nn\zeta}$ and $\theta_{\zeta\zeta n}$. When seen in the full context of $\mathrm{Re}(\mathcal{B}_{nn\zeta})$ and $\mathrm{Re}(\mathcal{B}_{n\zeta n})$ (figures 3*b* and 6*a*, respectively), this provides evidence for energy transfer arising from nonlinear wave–wave coupling between the magnetic potential and density fluctuations. Explicitly, magnetic potential fluctuations in the range 40–80 kHz exchange energy with density fluctuations the range 90–130 kHz. In all cases, this energy transfer is provided by the GAM frequency interacting with the broadband turbulent fluctuations.

5. Conclusion

Confirming the bicoherence interpretation of Melnikov *et al.* (2017*a*), the collaboration determined the indication of the energy transfer direction associated with specific

https://doi.org/10.1017/S0022377821000490 Published online by Cambridge University Press

groups of spectral features. We find that density, not electrostatic potential, fluctuations exhibit the best wave–wave coupling when paired with another fluctuating quantity. Magnetic potential fluctuations are also important to this coupling. Parents and daughters, characterized with Re($\mathcal{B}$), are present in the bispectrum of QC mode $f_{QC} \in [40, 150]$ kHz.

We recognize and report the signatures of three-wave coupling which provides evidence of energy transfer between density and magnetic potential through nonlinear interactions with GAM, supported by consistent features in Re($\mathcal{B}$) and non-random relationships between cross-biphases (e.g., $\theta_{nn\zeta}$ and $\theta_{\zeta\zeta n}$). Crucially, bicoherence involving the 17 kHz GAM is statistically meaningful, which implies the mode plays a dominant role in these wave–wave interactions, and reinforces the implied presence of nonlinear coupling. We also present evidence of the energy transfer direction associated with this three-wave coupling.

Acknowledgements

This work was supported by U.S. DoE (G.R., S.N., M.K., grant number DE-SC-0018036 and DE-SC-0020269) and the Russian Science Foundation (A.M., L.E., S.L., P.K., M.D., N.K., A.K., M.U., project number 19-12-00312). The work of A.M. was partly supported by the Competitiveness Program of NRNU MEPhI.

Editor Troy Carter thanks the referees for their advice in evaluating this article.

Declaration of interests

The authors report no conflict of interest.

REFERENCES

Conway, G.D., Angioni, C., Ryter, F., Sauter, P., Vicente, F. & ASDEX Upgrade Team 2011 Mean and oscillating plasma flows and turbulence interactions across the L-H confinement transition. *Phys. Rev. Lett.* **106**, 065001.

Cziegler, I., Tynan, G.R., Diamond, P.H., Hubbard, A.E., Hughes, J.W., Irby, J. & Terry, J.L. 2015 Nonlinear energy transfer in heated L-modes approaching the L-H transition in Alcator C-Mod. *Nucl. Fusion* **55**, 083007.

Demers, D.R., Schoch, P.M., Crowley, T.P., Connor, K.A. & Ouroua, A. 2001 Radial electrostatic flux inferred from core measurements of potential and density fluctuations. *Phys. Plasmas* **8**, 1278–1288.

Diamond, P.H., Itoh, S.I., Itoh, K. & Hahm, T.S. 2005 Zonal flows in plasma – a review. *Plasma Phys. Control. Fusion* **47**, R35.

Dnestrovskij, Y.N., Melnikov, A.V., Krupnik, L.I. & Nedzelskij, I.S. 1994 Development of heavy ion beam probe diagnostics. *IEEE Trans. Plasma Sci*. **22**, 310–331.

Eliseev, L.G., Melnikov, A.V., Lysenko, S.E., Khabanov, P.O., Zenin, V.N., Drabinskij, M.A., Kharchev, N.K., Kozachek, A.S., Krupnik, L.I. & HIBP Team 2018 Evaluation of turbulent particle flux by heavy ion beam probe in the T-10 tokamak. *Plasma Fusion Res*. **13**, 3402106.

Fujisawa, A., Ido, T., Shimizu, A., Okamura, S., Matsuoka, K., Iguchi, H., Hamada, Y., Nakano, H., Ohshima, S., Itoh, K., *et al.* 2007 Experimental progress on zonal flow physics in toroidal plasmas. *Nucl. Fusion* **47**, S718.

Gryaznevich, M., Stöckel, J., Van Oost, G., Del Bosco, E., Svoboda, V., Melnikov, A., Kamendje, R., Malaquias, A., Mank, G., Miklaszewski, R., *et al.* 2020 Contribution of joint experiments on small tokamaks in the framework of IAEA coordinated research projects to mainstream fusion research. *Plasma Sci. Technol*. **22**, 055102.

Jobes, F.C. & Hickock, R.L. 1970 A direct measurement of plasma space potential. *Nucl. Fusion* **10**, 195.

https://doi.org/10.1017/S0022377821000490 Published online by Cambridge University Press

KIM, Y.C., BEALL, J.M. & POWERS, E.J. 1980 Bispectrum and nonlinear wave coupling. *Phys. Fluids* **23**, 258–263.

KIM, Y.C. & POWERS, E.J. 1979 Digital bispectral analysis and its application to nonlinear wave interactions. *IEEE Trans. Plasma Sci*. **PS-7**, 120–131.

MELNIKOV, A.V. 2016 Applied and fundamental aspects of fusion science. *Nat. Phys*. **12**, 386–390.

MELNIKOV, A.V. 2019 *Electric Potential in Toroidal Plasmas*. Springer.

MELNIKOV, A.V., ELISEEV, L.G., JIMÉNEZ-GÓMEZ, R., ASCASIBAR, E., HIDALGO, C., CHMYGA, A.A., KOMAROV, A.D., KOZACHOK, A.S., KRASILNIKOV, I.A., KHREBTOV, S.M., *et al.* 2010 Internal measurements of Alfvén eigenmodes with heavy ion beam probing in toroidal plasmas. *Nucl. Fusion* **50**, 084023.

MELNIKOV, A.V., ELISEEV, L.G., LYSENKO, S.E., PERFILOV, S.V., SHURYGIN, R.V., KRUPNIK, L.I., KOZACHEK, A.S. & SMOLYAKOV, A.I. 2015*a* Radial homogeneity of geodesic acoustic modes in ohmic discharges with low *B* in the T-10 tokamak. *JETP Lett*. **100**, 555–560.

MELNIKOV, A.V., ELISEEV, L.G., LYSENKO, S.E., UFIMTSEV, M.V. & ZENIN, V.N. 2017*a* Study of interactions between GAMs and broadband turbulence in the T-10 tokamak. *Nucl. Fusion* **57**, 115001.

MELNIKOV, A.V., ELISEEV, L.G., PERFILOV, S.V., ANDREEV, V.F., GRASHIN, S.A., DYABILIN, K.S., CHUDNOVSKIY, A.N., ISAEV, M.Y., LYSENKO, S.E., MAVRIN, V.A., *et al.* 2013 Electric potential dynamics in OH and ECRH plasmas in the T-10 tokamak. *Nucl. Fusion* **53**, 093019.

MELNIKOV, A.V., ELISEEV, L.G., PERFILOV, S.V., LYSENKO, S.E., SHURYGIN, R.V., ZENIN, V.N., GRASHIN, S.A., KRUPNIK, L.I., KOZACHEK, A.S., SOLOMATIN, R.Y., *et al.* 2015*b* The features of the global GAM in OH and ECRH plasmas in the T-10 tokamak. *Nucl. Fusion* **55**, 063001.

MELNIKOV, A.V., KRUPNIK, L.I., ELISEEV, L.G., BARCALA, J.M., BRAVO, A., CHMYGA, A.A., DESHKO, G.N., DRABINSKIJ, M.A., HIDALGO, C., KHABANOV, P.O., *et al.* 2017*b* Heavy ion beam probing – diagnostics to study potential and turbulence in toroidal plasmas. *Nucl. Fusion* **57**, 072004.

MELNIKOV, A.V., VERSHKOV, V.A., ELISEEV, L.G., GRASHIN, S.A., GUDOZHNIK, A.V., KRUPNIK, L.I., LYSENKO, S.E., MAVRIN, V.A., PERFILOV, S.V., SHELUHKIN, D.A., *et al.* 2006 Investigation of geodesic acoustic mode oscillations in the T-10 tokamak. *Plasma Phys. Control. Fusion* **48**, S87.

RIGGS, G.A. 2020 Interpretations of bicoherence in space & lab plasma dynamics. MS thesis, West Virgina University.

STAUBER, R. 1995 Applicability of bispectral analysis to unstable plasma waves. MS thesis, West Virgina University.

STAUBER, R. & KOEPKE, M.E. 2021 Applicability of bispectral analysis to unstable plasma waves. *Plasma Phys. Control. Fusion* (submitted).

VERSHKOV, V.A., SARYCHEV, D.V., NOTKIN, G.E., SHELUKHIN, D.A., BULDAKOV, M.A., DNESTROVSKIJ, Y.N., GRASHIN, S.A., KIRNEVA, N.A., KRUPIN, V.A., KLYUCHNIKOV, L.A., *et al.* 2017 Review of recent experiments on the T-10 tokamak with all metal wall. *Nucl. Fusion* **57**, 102017.

VERSHKOV, V.A., SHELUKHIN, D.A., SUBBOTIN, G.F., DNESTROVSKIJ, Y.N., DANILOV, A.V., MELNIKOV, A.V., ELISEEV, L.G., MALTSEV, S.G., GORBUNOV, E.P., SERGEEV, D.S., *et al.* 2015 Density fluctuations as an intrinsic mechanism of pressure profile formation. *Nucl. Fusion* **55**, 063014.

XU, M., TYNAN, G.R., HOLLAND, C., YAN, Z., MULLER, S.H. & YU, J.H. 2009 Study of nonlinear spectral energy transfer in frequency domain. *Phys. Plasmas* **16**, 5195.